View metadata, citation and similar papers at core.ac.uk

brought to you by CORE

provided by NASA Technical Reports Server

DRA

OBJECTIVE SEA-LEVEL PRESSURE ANALYSIS FOR SPARSE DATA AREAS

By

Leonard M. Druyan

Institute for Space Studies

Goddard Space Flight Center, NASA

New York, New York 10025

October 1972

N73-18630

(NASA-TM-X-69135) OBJECTIVE SEA LEVEL PRESSURE ANALYSIS FOR SPARSE DATA AREAS (NASA) 41 p HC $4.25 CSCL 04B

Unclas G3/20 17266

ABSTRACT

A computer procedure, described in an earlier study, uses the wind speed field near the ocean surface in combination with a small number of observations of pressure and wind velocity to specify the maritime sea-level pressure field. An improved version was used to analyze the pressure distribution over the North Pacific Ocean for eleven synoptic times in February, 1967. Independent knowledge of the central pressures of lows is shown to reduce the analysis errors for very sparse data coverage. The application of planned remote sensing of sea-level wind speeds is shown to make a significant contribution to the quality of the analysis especially in the high gradient mid latitudes and for sparse coverage of conventional observations (such as over southern hemisphere oceans). Uniform distribution of the available observations of sea-level pressure and wind velocity yields results far superior to those derived from a random distribution. A generalization of the results indicates that the average lower limit for analysis errors is between 2 and 2.5 mb based on the perfect specification of the magnitude of the sea-level pressure gradient from a known verification analysis (A less than perfect specification will derive from wind-pressure relationships applied to satellite observed wind speeds.) and fifteen uniformly distributed, high quality bouy, weather ship or island observations of the pressure and

wind velocity. Analysis errors computed using poorly defined wind fields indicate the procedure's potential for sparse data analysis even without supplementary satellite data.

II

1. Introduction

A previous report by the author (Druyan, 1972) has described a computer procedure for the analysis of maritime sea-level pressure and wind fields. The method is an application of the satellite system proposed by Moore and Pierson (1970) for the remote measurement of the sea-level wind speed.

This report is based on an improved version of the procedure; it discusses the analysis sensitivity to the quality and distribution of conventional observations and the qualtiy of the pressure gradient specification.

Research is continuing on the experimental and theoretical aspects of using active microwave radar and passive radiometry in order to measure the energy in that portion of the ocean wave spectra which is the most sensitive to the local wind (Pierson and Moore, 1972; Pierson, et. al, 1971). A prototype instrument will be operated from the manned orbiting satellite, Skylab, and may collect data of this type from space for the first time in the Spring of 1973.

Better specification of the sea-level pressure and wind fields has obvious applications to ocean wave forecasting and weather forecasting for coastal regions. In addition, the combination of satellite

derived temperature profiles with sea-level pressures can serve to improve the specification of upper pressure surfaces through the hydrostatic formulation. Several numerical simulation studies also indicate that wind errors may be more effectively reduced by inserting temperature profile data in combination with sea-level pressures rather than with pressure data from a near tropopause level (Kasahara and Williamson, 1972; Jastrow, 1972). Moreover, because of the vast ocean areas of the southern hemisphere, supplying surface pressures only over land gives considerably larger circulation errors than when the entire reference pressure field is specified (Jastrow, 1972).

2. General discussion of experiments

A large number of observations of sea-level wind and pressure (hereafter referred to as the conventional observations) over the North Pacific Ocean were gathered from non-real-time sources to supplement data normally available at map time. [A discussion of the availability and reliability of these data is found in Cardone (1969).] A horizontal interpolation of the wind field according to Cardone's model of the marine boundary layer yields a gridded array of wind speeds consistent with the 200 or more conventional observations of a given map time (see Appendix). These speeds are used to simulate the pattern of wind speed data that would become routinely available should the proposal of Moore and Pierson prove feasible.

[A more detailed discussion of the simulation of the satellite observed data and the recovery of the entire wind speed field is found in Druyan (1972).]

The input for each analysis is a small number of conventional meteorological observations, the location of low pressure centers and the extensive specification of the sea-level wind speed field. The procedure uses the wind speed in order to estimate the pressure gradient magnitude, and the pressure field is extrapolated outward from the low pressure centers and the convential observations.

Persistence or even climatology often provides a realistic analysis of the sea-level pressure field in the tropics. On the other hand, extrapolating the mid-latitude pressure analysis to very low latitudes using wind-pressure relationships is a precarious venture. Unfortunately, the grid by grid specification of such tropical pressures are tedious to prepare for the particular grid system used in this study. Therefore, observations from eight tropical stations, some corresponding to islands, one to weather ship N and the others estimated from the real-time NMC Northern Hemisphere analysis were used as permanent input data. An observation was also added in each case in the area of Los Angeles, Calif. because a considerable number of grid points lie over the western United States.

In order to integrate the analysis with the coastal pressure observed by continental stations, pressures are made available to the analysis along the northernmost "i" grid line (see Fig. 1), and three horizontal rows of pressure are interpolated between these border values and those from within the analysis

The boundary data and the trpoical observations are referred to as the "permanent data" in the discussion below.

The central pressure of each low acts as a seed in determining the value of the pressures within its area of influence. Each such pressure minimum is computed as the distance weighted average of estimates derived from conventional pressure and wind velocity observations and/or northern boundary pressure values that are located within some scan radius from the low pressure center. The analysis procedure modifies the initially symmetric pattern of pressures increasing radially outward from each low center by causing the isobars to separate or come together in conformity with the speed implied magnitude of the pressure gradient.

Similarly, the analysis in the vicinity of an observing station uses the observed pressure as the seed value; the total pressure gradient at the point of observation is determined by the wind velocity. The procedure extends the analysis outward from each such observation by allowing the

the isobar spacing to adjust to the wind derived pressure gradient magnitude at each surrounding grid point.

The procedure has been slightly improved since the initial results were published in Druyan, 1972. A significant amount of computer program debugging has eliminated the infrequent appearance of spurious pressures at several grid points in the analysis. Further, whereas it was earlier reported that the sub-tropical high pressure ridges were located by searching for the highest pressure observation in each low pressure system quadrant, the newer version predesignates the latitude of this ridge by climatological considerations. Other high pressure centers result either from a corresponding pressure observation or from the relative maximumum created between two adjacent low pressure systems.

A pressure field derived from all of the available conventional observations at a given map time is used as the standard for the verification of a sparse data analysis; grid by grid pressures are compared and the RMS difference between the two fields is referred to as the analysis error.

It was found that, for the purposes of creating a smooth pressure field for verification consistent with a high density of observations (see, for example, Fig. 1), an analysis method different from the procedure under discussion (which shows promise for situations of very sparse observational coverage) was desirable. The pressures for each verification field are

assigned by taking a distance weighted average of estimates computed for each grid point from the pressure and wind observations within some scan radius from the grid point. In addition to improving the all-data map, the new procedure also makes the verification more meaningful because the fields to be compared are created by independent procedures.

Sea-level pressure analyses for the North Pacific Ocean (see Fig. 1) were made for eleven synoptic times in February, 1967 using in each case the permanent data and either all of the available conventional observations or a data set representing a sparse network of observations. The analysis error was computed each time and averaged over the eleven maps for each experiment.

3. Sensitivity to Central Pressure

Since the analysis technique uses the low pressure centers as starting points for much of the extrapolation, the objective estimate of the central pressures is crucial to the accuracy of the resulting field. Under operational circumstances the central pressure can often be estimated from extrapolation in time to within a few millibars accuracy; otherwise on-time observations from nearby land or maritime stations are needed to make these estimates.

In order to determine the extent to which a "perfect" knowledge of the central pressures can improve the accuracy of the analysis,

the eleven pressure fields were generated with various distributions of the conventional meteorological network and the values of the pressure minima specified externally. (Those computed for the corresponding maximum data analyses were used.) Figure 2 shows the two graphs of the average analysis errors for the eleven synoptic times plotted as a function of the number of uniformly distributed conventional observations, one for the analyses which were supplied with the central pressures and the other for the analyses which computed these values internally. Although the average analysis error can be reduced by as much as 1 mb by supplying the values of the pressure minima to analyses based on five meteorological stations over the area, the advantage almost disappears when as many as 15 well-deployed stations are available. In the latter circumstance, the objective determination is quite adequate.

4. Sensitivity to the pressure gradient formulation

Given a "perfect" estimate of the central pressure and the magnitudes of the pressure gradient, any remaining deficiencies of the resulting analysis are due to inadequacies in the objective parameterization of the gradient direction. A "perfect" field was specified for each of the eleven synoptic times by using the analysis of the hundreds of conventional meteorological observations

as discussed above; "perfect" central pressures and pressure gradients were thus created from these fields.

Each of the eleven fields was recovered using these central pressures and gradients as well as the permanent data, but with none of the original conventional observational data. The results were compared to the original all-data fields by computing the RMS difference between their pressures at corresponding grid points. The average analysis error for the eleven maps is 3.2 mb. This "residual" error can be directly attributed to errors in the gradient direction which is not explicitly assigned at each grid point; it is of course independent of errors in the magnitude of the gradients and errors in the "seed" or "anchor" pressures. On the other hand, the inclusion of the conventional observations as in many of the analyses discussed below somewhat limits the extent of errors caused by estimates of the gradient direction.

The pressure gradient magnitudes were then computed by objectively analyzed wind speeds according to the formulation discussed in detail in the original study cited above (see also Appendix). The average analysis error for the same eleven fields analyzed as before save for the use of the wind speeds in the computation of the gradients, was slightly more than $\frac{1}{2}$ mb larger than that computed above for the perfect gradient analyses. Thus, if these maps are representative of winter

situations, it may be concluded that the analysis is degraded by about $\frac{1}{2}$ mb in the RMS sense due to the derivation of the pressure gradient magnitude from even a well specified wind speed field as compared to the ideal specification of "perfect" gradients. Limitations in the objective wind analysis of Cardone (1969) and in the particular calculation of the pressure gradient magnitude [the equations, which were reported in the original study (Druyan, 1972), represent a series of step functions and thus depart from Cardone's intended formulation of the dependence of the observed wind on pressure gradient, air-sea temperature difference and latitude (see Appendix)] can eventually be overcome and may thus contribute to a reduction of this particular source of error.

The scheme whereby the wind speed is used to compute the magnitude of the pressure gradient involves an iteration of the pressure analysis. The pressure field after the first iteration is used to compute isobar curvature which modifies the previously determined pressure gradients before the second iteration of the analysis is executed. In order to determine whether or not the time-consuming iteration makes a significantly positive contribution to the accuracy of the analysis, the eleven fields were verified before the second iteration in which the pressure gradients are modified by curvature. The average analysis error computes to more than $\frac{1}{2}$ mb higher than when the effect of curvature is included.

The experiment was repeated with yet another formulation of pressure gradient magnitude. A set of random wind speed errors was generated whose standard deviation was 4.6 kt. These were used to contaminate the wind speed field in random fashion by adding or subtracting them from the objectively analyzed values used in the previous experiment. The resulting "degraded" wind speeds were then used as before to compute the pressure gradient magnitudes. The average analysis error of the resulting eleven sea-level pressure fields was 4.0 mb, about 0.8 mb greater than that incurred by using perfect pressure gradients and only about 0.25 mb greater than that incurred by using the original wind speed analysis. Undoubtedly the smoothing of the final field eliminates much of the error produced by the random contaminations. It is also probable that the original wind speed field contained its own random errors.

In order to determine the analysis errors that would result from a "worst guess" wind speed specification, the eleven sea-level pressure fields were analyzed by assuming a wind speed at every grid point of 15 kt and computing the pressure gradient as before. Thus, the pressure gradient magnitudes varied only according to latitude (due to the latitudinal dependence of the Coriolis parameter) and air-sea temperature difference (see Druyan, 1972). The average analysis error of the resulting fields was 5.5 mb which

is almost 2 mb (48%) higher than that resulting from the well-specified wind speeds and about 2.3 mb greater than that incurred by the perfect pressure gradient formulation. Accounting for curvature provided no significant systematic improvement in the analyses based on 15 kt wind speed.

It should be noted that the average analysis errors given above include the well specified (by the permanent data), low-gradient tropics as well as the high-gradient mid-latitude regions. The errors are always lower in the former and larger in the latter area than the RMS values computed for the entire field. Also, the deterioration due to a less realistic pressure gradient formulation is more pronounced in the mid-latitudes than in the tropics. The average RMS error computed for only the northern half of each map is given for the different formulations of the pressure gradient.

Perfect pressure gradient:	3.5 mb
Well-specified wind speeds:	4.3 mb
Well-specified wind speed, no curvature:	4.9 mb
Perturbed wind speeds:	4.7 mb
Uniform 15 kt wind speeds:	6.8 mb

Fig. 3 shows five sample sea-level pressure analyses based on each of the above formulations of the pressure gradient. (There is a considerable distortion in these computer drawn maps which have

stretched the vertical dimension relative to the horizontal. For a true representation of the field dimensions see Fig. 1.) Also shown is the verification map (3a) which represents the analysis of about 250 ships' observations for 00Z, 8 February 1967. The analysis which assumed the perfect pressure gradients (3b) has reproduced the actual field to a remarkable extent considering how few pressure values were supplied externally (the permanent data and the central pressures of lows). On the other hand, the analysis which assumed a 15 kt wind speed at each grid point (3f) has distorted the pattern on the western side of the low pressure trough, has completely missed the narrow ridge in the west and has grossly overestimated the pressures at the upper left edge.

Of the three remaining charts in Fig. 3, the one which used the well-specified wind speed field and corrected for curvature (3c) came the closest to building the narrow ridge in the west to proper strength. The analysis for which curvature was neglected (3d) is slightly inferior to that of 3c. The analysis which used the contaminated wind speeds (3e) erroneously widened the trough between the two low centers and completely missed the short wave ridge outlined by the 1004 mb isobar on all of the other maps northeast of the elongated low pressure trough. All three of these maps missed the ridging in the east.

Fig. 4 shows three graphs of the average analysis errors of the eleven synoptic times computed for the northern half of the analysis area and plotted as a function of the number of uniformly distributed conventional observations for different formulations of the pressure gradient. The perfect pressure gradient derived analyses verify with lower average errors than those based on the wind speed field at all observational network sizes. The deterioration of the analysis quality is of course much more pronounced when uniform wind speeds of 15 kt are assumed.

6. Sensitivity to the qualtiy and distribution of conventional observations

The sensitivity of the analysis to the quality and distribution of the conventional meteorological observations was tested. The maximum data analyses were used to simulate "perfect" observations of sea-level pressure and wind velocity at designated grid points. These grid points represent a plausible buoy or ship network at which the meteorological observations are assumed to be of high quality.

Any given number of observations was deployed in one of three alternative distributions: a network representing uniform (within the limitations of the number) buoy coverage of the non-tropical areas, a northern shift which concentrated the stations in the northern third

of the field but nevertheless maintained uniform spacing between them and a random distribution where uniform spacing was not guaranteed. The eleven sets of analyses were completed by using each of the observational networks in combination with the well-specified wind speed fields; the pressure minima were computed objectively from the available data. The average analysis errors incurred by each network for the eleven maps are plotted as a function of the number of observations as shown in Figure 5.

The use of the uniform distribution of buoys resulted in consistently superior analyses although the central pressure was determined objectively by the model. The advantage afforded the central pressure computation by the high density of observations in the region of maximum cyclone activity provided by the northern-most distribution as well as the strategic value of having more observations over the high gradient region were apparently offset by data voids elsewhere.

Coordinates were chosen by random selection in order to represent a network of ships whose meteorological observations are of superior quality. These latter were simulated in the same manner as the "bouy" observations above. In each of three independent random selections of fifteen observations, the first five, the first ten and all fifteen were each respectively designated as observational networks.

The average analysis error for the eleven maps for a given number of "ships" was averaged for the three different randomly picked distributions. The analysis errors were consistently higher than their counterparts computed from a uniformly distributed network of bouy observations (see Fig. 5). The considerable variability observed in the quality of these analyses indicates the extreme sensitivity of the procedure to the deployment of conventional observations.

Three independent random picks were made of fifteen actual ship reports, each from the entire list of observations available for each of the eleven maps. As before, their deployment over the analysis area is also completely random but, in this case, it varies from map to map. All fifteen observations, the first ten and the first five for each of the three random selections determined an observational network for analysis. Whereas the simulated observations were derived from each smooth all-data "perfect" analysis, the individual ships' observations of sea-level pressure and wind are sometimes less representative of the "perfect" analysis against which the results are verified. This "perfect" pressure field represents the integration of data from a high density network and as such, the impact of any one observation that is "out of step" with the majority in its vicinity is diminished.

However, when such an observation is used in a sparse data analysis, its sphere of influence is quite extensive.

As before, the average analysis error for the eleven maps for each of the three network sizes was averaged for the three different random selections. The grand average RMS obtained for the fifteen ship network is 4.0 mb; for the ten ship network it is 4.2 mb; for the five ship network it is 6.0 mb. (See Fig. 5.)

The results reflect sensitivity of the analyses to the randomness of the distribution and to the non-representativeness of some of the observations. Because of the latter these analyses are inferior to those obtained for the random distribution of "perfect" observations and they are more inferior yet when compared to the "perfect" and uniform distribution derived maps.

7. Conclusions

Sea-level pressure fields generated by the procedure are shown to be of higher quality when the pressure at the low centers is supplied externally in combination with five uniformly distributed, perfect observations of the pressure and wind than when these pressure minima are computed internally. However, this advantage disappears when as many as fifteen observations are used.

The computation of the pressure gradient from a well-specified wind speed field, which could become a routine product of satellite observation if current research bears fruit, yields analyses which are, on the average, superior to those which are deprived of the wind speed specification. This deterioration is reflected by an increase in the average analysis error for the northern half of 2.5 mb in those charts which were generated from the "seed" pressures at the low centers. The amount of the error increase due to poor wind speed specification is somewhat diminished by pressure observations which correct the analysis wherever they are made available. Smoothing of the pressure analysis greatly reduces the impact of random errors in the wind speed field and thus the charts generated from such fields are only slightly inferior to those based on a good wind speed specification. Accounting for curvature by iterating the analysis a second time appears to have a significantly positive effect except when the uniform speeds are used. The improvement in the analyses resulting from specifying perfect pressure gradient magnitudes indicates that better results can be expected from more representative wind speed fields and better transformation from wind speeds to pressure gradients.

Uniform spacing of the observation network is shown to be far superior to the use of random maritime observations even when the latter are of high reliability; the case for meteorological buoy stations is obvious.

The rather small RMS errors computed for the northern half of the field (see Fig. 4) with just ten or fifteen observations suggests the model's possible application to sea-level pressure analysis in sparse data regions even without the availability of satellite observed wind speeds. The analyses based on 15 kt yield an upper limit to the error since some climatological guess of the wind field should be superior to the uniform speed assumption. Traditional analysis procedures depend on a sometimes poor initial guess field which is barely modified in data sparse regions whereas the one described herein constructs a completely new field by the interpolation between and extrapolation from known observations. Lewis and Grayson (1972) have demonstrated how a low error initial guess field can be improved by considering supplemental wind data, but, the construction of a new pressure field, consistent with the available wind data as described above, provides a promising alternative to the traditional correction methods.

The isobar orientation implies a wind direction and, in combination with an observed wind speed field, defines the total wind vector. Investigation into the specification of the sea-level wind velocity derived from the sparse data analyses is proceeding and application of the results to ocean wave forecasting will be considered.

Acknowledgements. Research described in this study was performed during the author's tenure as Research Associate with the support of the National Academy of Science, National Research Council. The facilities provided by Dr. Robert Jastrow at the Goddard Institute for Space Studies are gratefully acknowledged. The author is indebted to Professor W. J. Pierson of New York University for his continuous interest and encouragement of the research. The author would also like to thank Professor V. J. Cardone of New York University for his help in the preparation of the appendix.

APPENDIX

Summary of the Cardone (1969) Marine Boundary Layer Model

1. The relationship between the geostropic and actual sea-level winds.

The Cardone formulation is an extension of Blackadar's (1965) two-layer modeling of the boundary layer wind profile. It assumes a constant flux layer in which the eddy viscosity variation with height is specified as a function of the atmospheric stability according to the Monin-Obukov similarity theory and an upper layer which incorporates an Ekman profile with a constant eddy viscosity. The characteristics of the lower boundary are prescribed internally by a functional relationship between the roughness parameter Z_o (cm) and the friction velocity U_* (cm sec^{-1}):

$$Z_o = .684/U_* + 4.28 \times 10^{-5} U_*^2 - 4.43 \times 10^{-2}$$

The following set of simultaneous equations relating the geostrophic wind (G) and the air-sea temperature difference $(\theta_a - \theta_s)$ with the stability length (L′), the cross-isobar angle of the wind vector (Ψ_o) and U_* are solved by numerical iteration:

$$L' = U_*^2 \bar{\theta} [\ell n(Z_a/Z_o) - \Psi(Z_a /L')]/K^2 g(\theta_a - \theta_s)$$

$$U_* = G[2K B_o \sin^2 \Psi_o \phi_u (h/L')]^{1/2}$$

$$U_* = GK\sqrt{2} \sin(\pi/4 - \psi_o)/[\ell n B_o R_o - \Psi(h/L')]$$

where h, the height of the top of the lower layer is given by $B_o G/F$ and

B_o, a dimensionless constant, is equal to 3.0×10^{-4} ,

F is the Coriolis parameter $2\Omega \sin(\text{LAT})$,

R_o is the surface Rossby number G/FZ_o ,

K is VonKarman's constant (≈ 0.4)

Z_a is the height above the sea surface at which θ_a is taken,

and $\bar{\theta}$ is the mean potential temperature of the boundary layer.

$\phi_u (h/L')$ is the non-dimensional wind shear given by

$1 + \beta' (h/L')$ for stable conditions (i.e., $\theta_a > \theta_s$); by the implicit so-called KEYPS function (Panofsky, 1963) for unstable conditions,

$$\phi_u^4 - \gamma' h/L' \phi_u^3 - 1 = 0$$

and $\phi_u = 1$ for neutral conditions.

The constants, β' and γ' are estimated to be 7 and 18 respectively).

$\psi(Z/L')$ is the integrated non-dimensional wind shear which is evaluated as follows:

$$\psi(Z/L') = \int_0^{Z/L'} [1 - \phi_u(\xi)]/\xi \, d\xi$$

The wind speed at 19.5 m above the sea surface is

$$U_{19.5} = (U_*/K)\, \ell n 19.5/Z_o \quad .$$

The direction of the wind is found at Ψ_o degrees from the geostrophic direction.

Thus, the wind vector at 19.5 m is determined by a numerical iteration from some first guess values of U_* and Ψ_o as well as the computed geostrophic wind and air-sea temperature differences.

The problem of determining the pressure gradient from satellite observations of the sea-level wind speed (The author takes $U_{19.5}$ to represent the sea-level wind speed.) is the inverse of the Cardone procedure. Thus, the linear relationships presented in Table 1. of Druyan (1972) represent best fits to a wide range of values of $U_{19.5}$ vs G generated over a range of air-sea temperature differences and latitudes by Cardone's scheme.

2. The objective interpolation of the sea-level winds.

The procedure described above assigns a wind at each point in a field based on the analyses of sea-level pressure and air-sea temperature difference. It is desirable to correct the analysis with observations of the wind that might be available not only at the grid points corresponding to them but also at surrounding points to insure a realistic and smooth field.

Cardone uses the Conditional Relaxation Analysis Method developed by Harris, Thomasell and Welsh (1966) to integrate the wind observations with those derived from the pressure and temperature field. The latter serve as both boundary values along the edge of the grid array to be computed and as the initial guess field within the array which determines the forcing function for the relaxation. The relaxation is made for the two orthogonal wind components seperately and the grid values are required to satisfy Poisson's equation,

$$\nabla^2 u(i,j) = F_u(i,j)$$

$$\nabla^2 v(i,j) = F_v(i,j)$$

subject to the constraints of the observations of u and v acting as internal boundary points. $F_u(i,j)$ and $F_v(i,j)$, the forcing functions, define the shape of the u and v fields respectively and are computed to be the Laplacian at each (i, j) of the initial guess u and v fields.

For the purposes of this study, such objective wind analyses were converted to gridded arrays of the wind speed which were used to simulate satellite observed winds within the sub-satellite swaths.

LIST OF FIGURES

Fig. 1. Extent of area under study. The borders of the cartesian grid system are represented and the dots indicate the locations of the maritime observations collected for 8 February 1967.

Fig. 2. Average analysis errors for eleven synoptic times in February, 1967 plotted as a function of the number of uniformly distributed observations. The analyses represented by both curves used well-specified wind speed fields in order to compute the pressure gradient, but one set (X) was supplied with perfect central pressures while the other (O) computed them internally.

Fig. 3. The sea-level pressure fields for 8 February 1967 isoplethed automatically and objectively analyzed:

a) for about 250 actual ship observations of pressure and wind; with perfect central pressures and
b) perfect pressure gradients; analysis error = 2.2 mb.
c) a well-specified wind speed field; analysis error = 2.7 mb.
d) same as c) but neglecting curvature; analysis error = 3.5 mb.
e) a wind speed field degraded by random errors; analysis error = 3.0 mb.
f) a uniform wind speed of 15 kt; analysis error = 5.1 mb.

(Note that the vertical dimension has been stretched in these computer generated representations.)

Fig. 4. Average analysis errors for the northern half plotted as a function of the number of uniformly distributed observations. The eleven sea-level pressure fields are the same as those whose analysis errors are shown in Fig. 2, but the central pressures have in every case been computed internally and the pressure gradient has been either specified from the corresponding "perfect" analyses (X), computed from well-specified wind speeds (O) or computed by assuming 15K wind speed everywhere (Δ).

Fig. 5. Average analysis errors for the eleven maps plotted as a function of the number of observations. All analyses computed the pressure minima internally and the pressure gradients from well-specified wind speed fields. The observations simulate a uniform network of buoy stations (X), a northern shift network of buoy stations (O) and a random distribution of high quality ship observations (Δ); the ramaining curve (•) shows the average analysis errors resulting from the random distribution of actual ship observations.

REFERENCES

Blackadar, A.K., 1965: A simplified two-layered model of the baroclinic neutral atmospheric boundary layer. Final Report: Flux of Heat and Momentum in the Planetary Boundary Layer of the Atmosphere. Penn. State University.

Cardone, V., 1969: Specification of the wind distribution in the marine boundary layer for wave forecasting. GSL Report. TR-69-1, Department of Meteorology and Oceanography, New York University.

Druyan, L., 1972: Objective analysis of sea-level winds and pressures derived from simulated observations of a satellite radar-radiometer and actual conventional data. Jnl. of Appl. Met., 11, 413-428.

Harris, R.G., A. Thomasell, and J. Welsh, 1966: Studies of techniques for the analysis and prediction of temperature in the ocean. Part III, Automated Analysis and Prediction. Report 7421-213, Travelers Research Center, Inc.

Jastrow, R., 1972: Observing system simulation studies. (submitted to Bull. Amer. Meteor. Soc.)

Kasahara, A. and D. Williamson, 1972: Evaluation of tropical wind and reference pressure measurements-numerical experiments for observing systems. Tellus, 24, 100-115.

Lewis, J. and T. Grayson 1972: The adjustment of surface wind and pressure by Sasaki's variational matching technique. Jnl. of Appl. Met., 11, 585-597.

Moore, R. and W. Pierson, 1970: Worldwide oceanic wind and wave predictions using a satellite radar-radiometer. AIAA Paper No. 70-310.

Panofsky, H.A., 1963: Determinations of stress from wind and temperature measurements. Quart. J. Roy. Meteor. Soc., 89, 85-94.

Pierson, W. and R. Moore, 1972: The extrapolation of laboratory and aircraft radar sea return data to spacecraft altitudes. In Proc. of Fourth Annual Earth Resources Review, MSC, Houston, Texas (in press).

Pierson, W.; Jackson, F.; Stacy, R. and E. Mehr, 1971: Research on the problem of the radar return from a wind roughened sea. Advanced Applications of Flight Experiments-Principle Investigators' Review, NASA Langley Research Center, pp. 83-114.

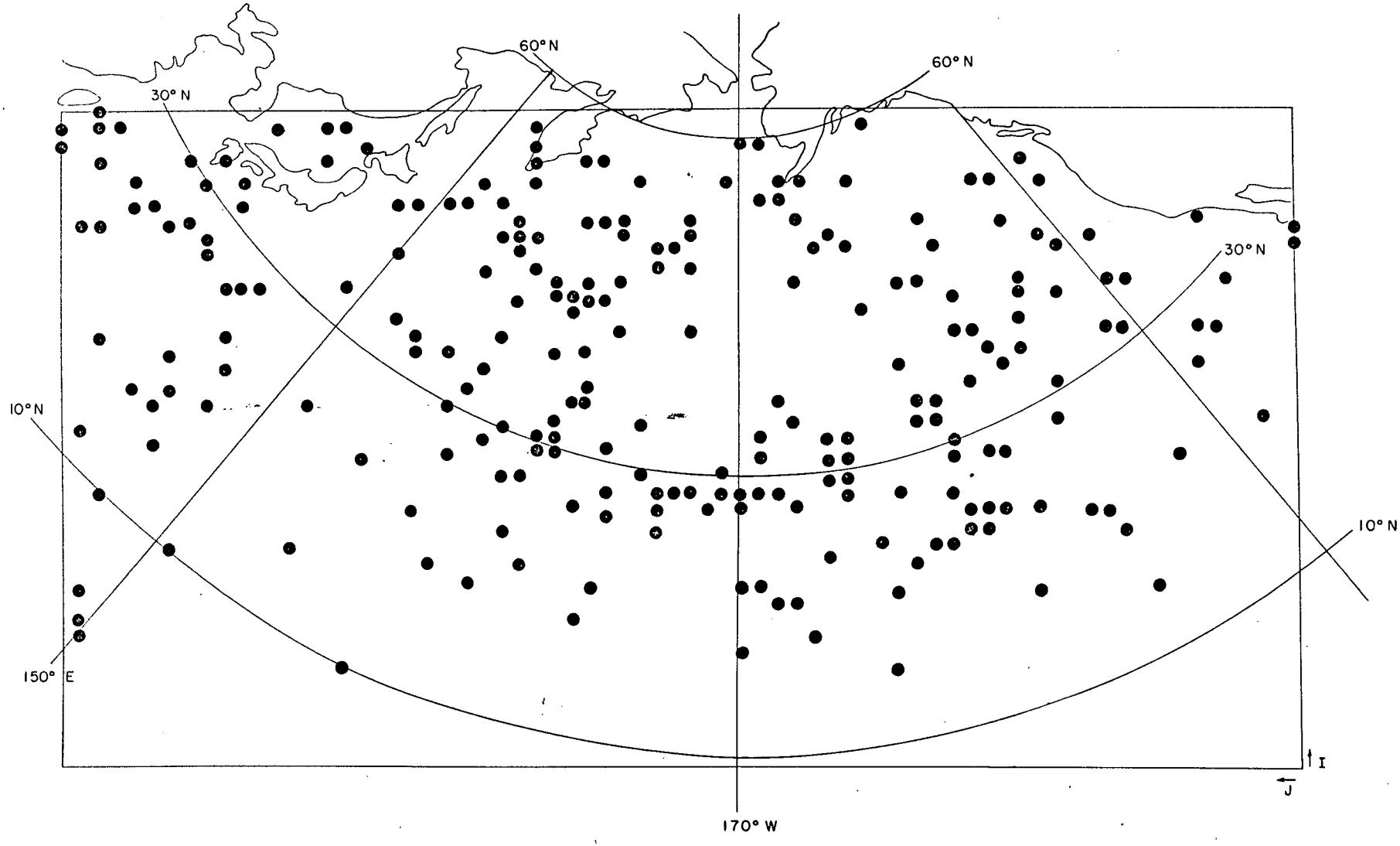

d-8977

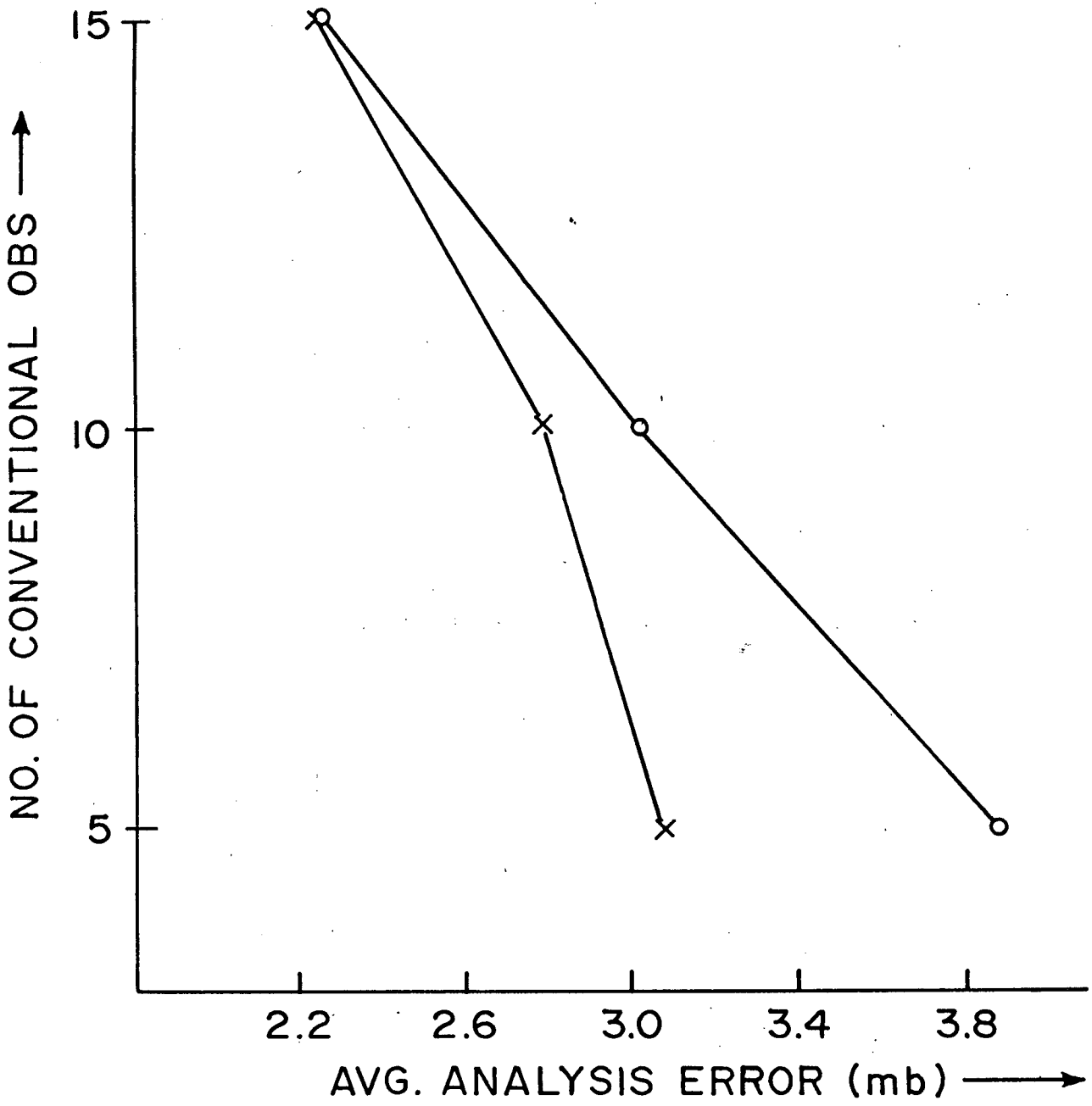
15
10
5
NO. OF CONVENTIONAL OBS
2.2
2.6
3.0
3.4
3.8
AVG. ANALYSIS ERROR (mb)

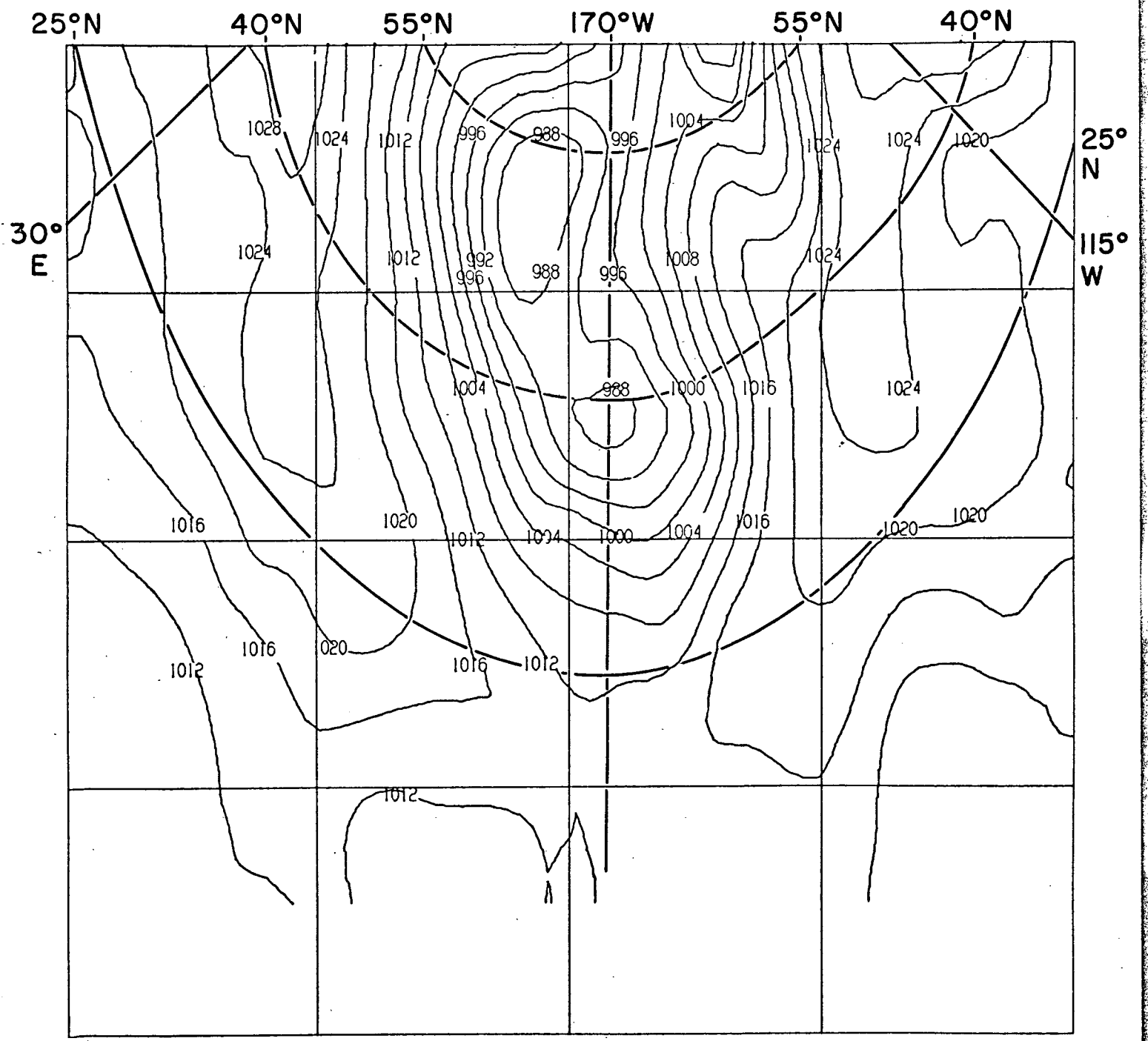
25°N
40°N
55°N
170°W
55°N
40°N
25°
N
115°
W
30°
E
1028
1024
1012
996
988
996
1004
1024
1024
1020
1024
1012
992
996
988
996
1008
1024
1004
988
1000
1016
1024
1016
1020
1012
1004
1000
1004
1016
1020
1020
1016
020
1012
1016
1012
1012

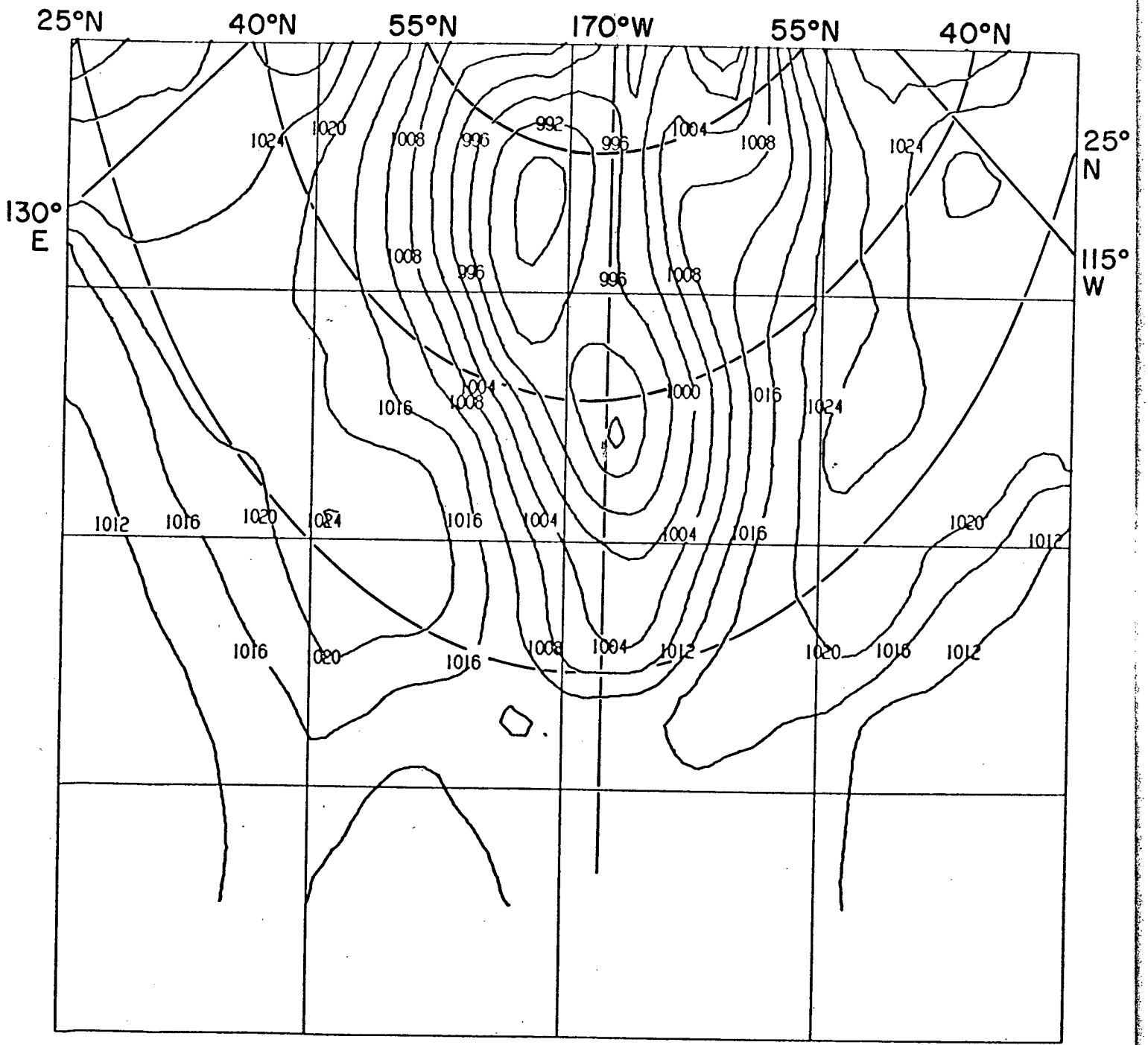
25°N
40°N
55°N
170°W
55°N
40°N
25° N
115° W
130° E
1024
1020
1008
996
992
996
1004
1008
1024
1008
996
996
1008
1004
1000
1016
1024
1016
1008
1012
1016
1020
1024
1016
1004
1004
1016
1020
1012
1016
1020
1016
1008
1004
1012
1020
1016
1012

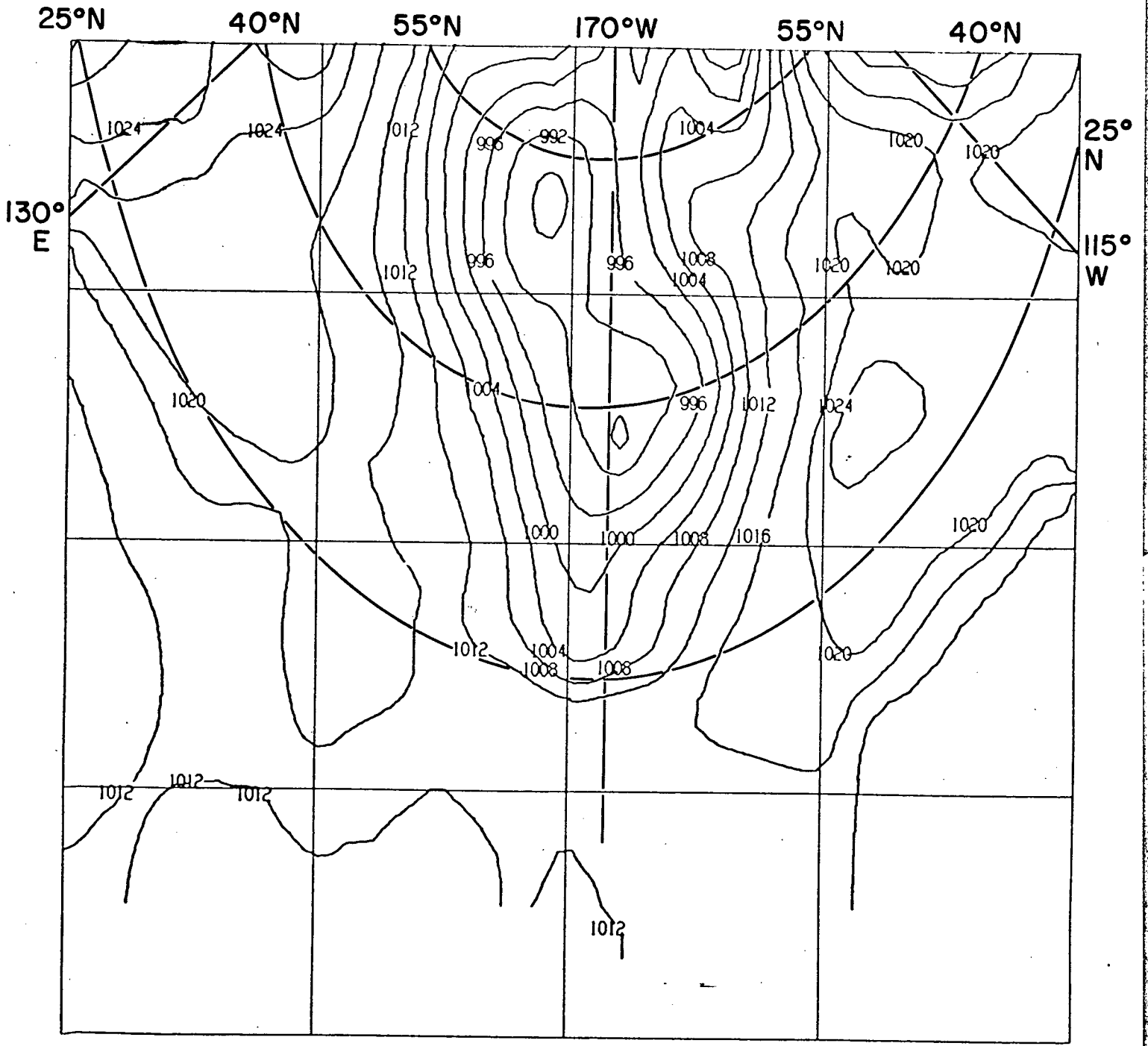
25°N
40°N
55°N
170°W
55°N
40°N
25°
N
130°
E
115°
W
1024
1024
1012
996
992
1004
1020
1020
1012
996
996
1008
1004
1020
1020
1020
1004
996
1012
1024
1000
1000
1008
1016
1020
1012
1004
1008
1008
1020
1012
1012
1012
1012

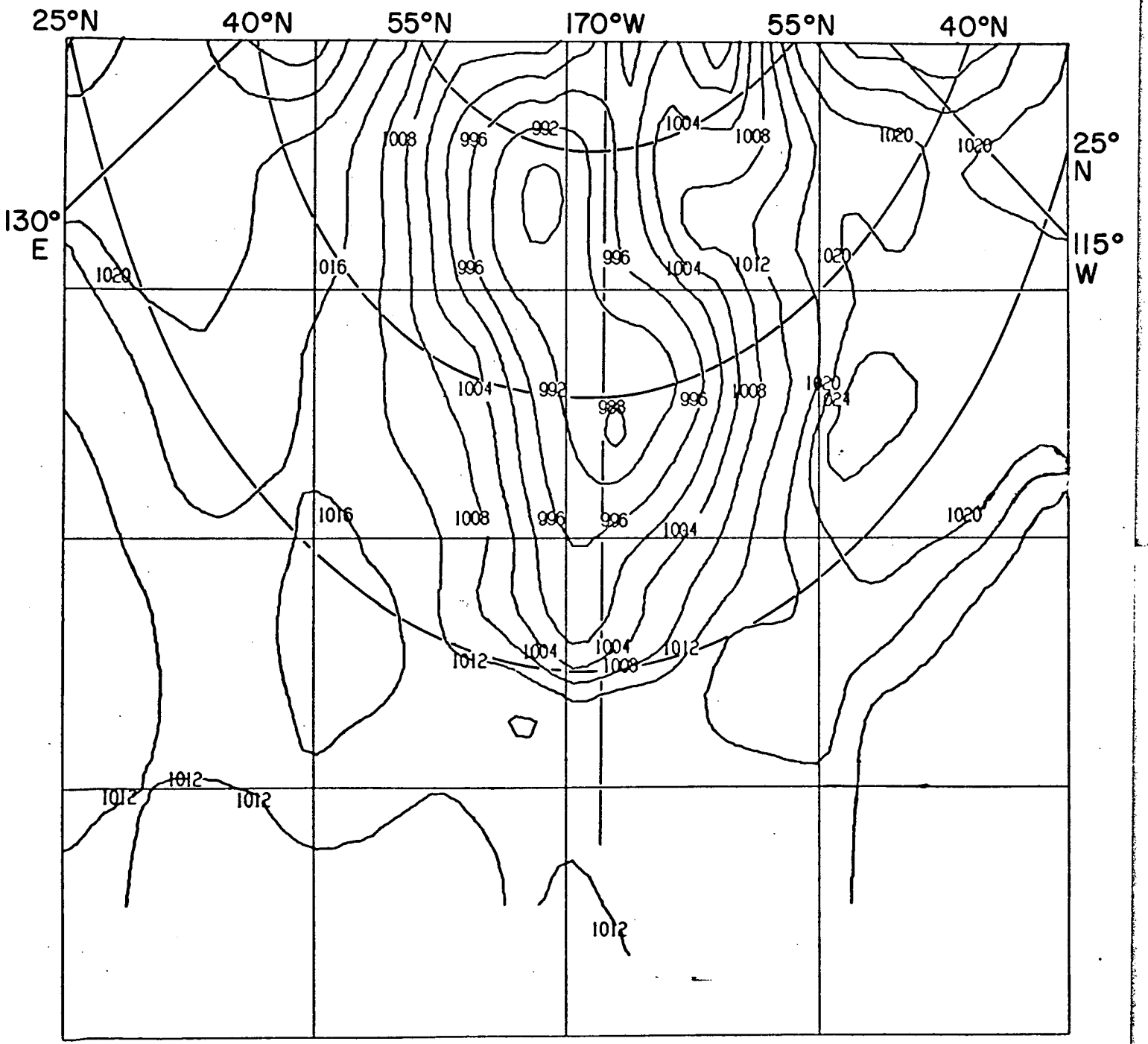
25°N
40°N
55°N
170°W
55°N
40°N
25°
N
130°
E
115°
W
1008
996
992
1004
1008
1020
1020
1020
016
996
996
1004
1012
020
1004
992
988
996
1008
1020
024
1016
1008
996
996
1004
1020
1012
1004
1004
1012
1008
1012
1012
1012
1012

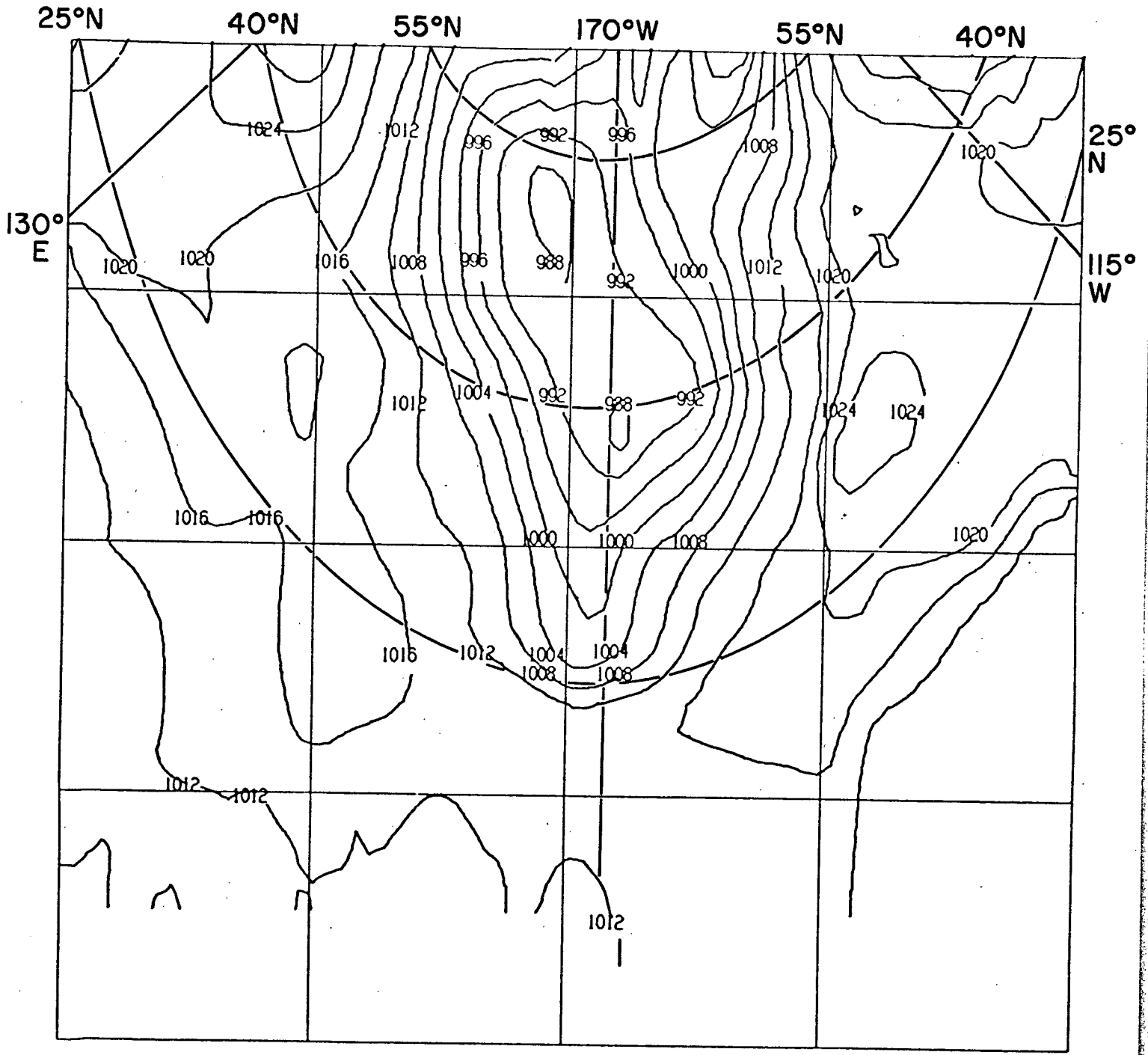
25°N
40°N
55°N
170°W
55°N
40°N
130° E
25° N
115° W
1024
1012
996
992
996
1008
1020
1020
1020
1016
1008
996
988
992
1000
1012
1020
1012
1004
992
988
992
1024
1024
1016
1016
1000
1000
1008
1020
1016
1012
1004
1004
1008
1008
1012
1012
1012

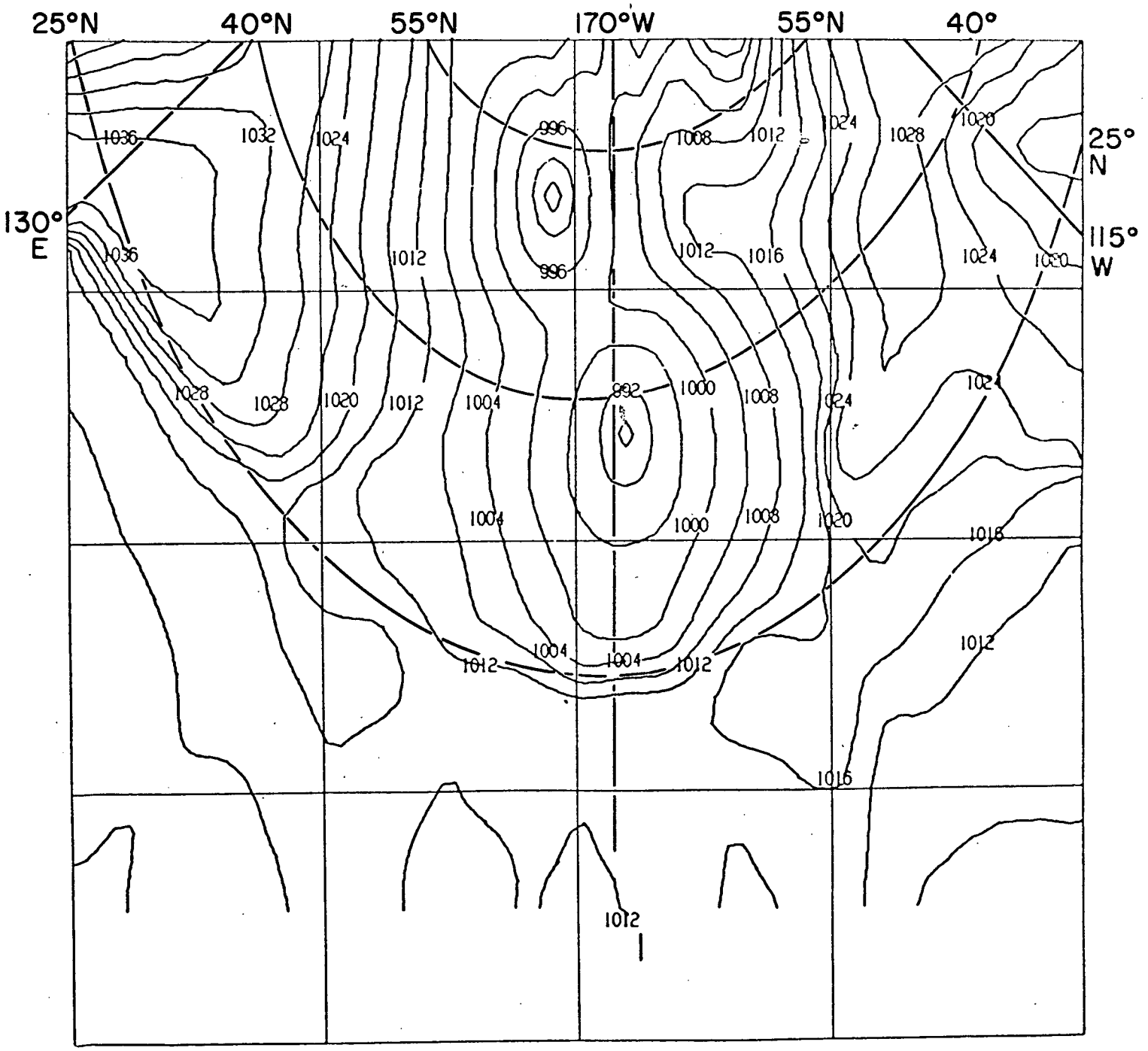
25°N
40°N
55°N
170°W
55°N
40°
25° N
130° E
115° W
1036
1032
1024
996
1008
1012
1024
1028
1020
1036
1012
996
1012
1016
1024
1020
1028
1028
1020
1012
1004
992
1000
1008
024
1024
1004
1000
1008
1020
1016
1012
1004
1004
1012
1012
1016
1012

3f

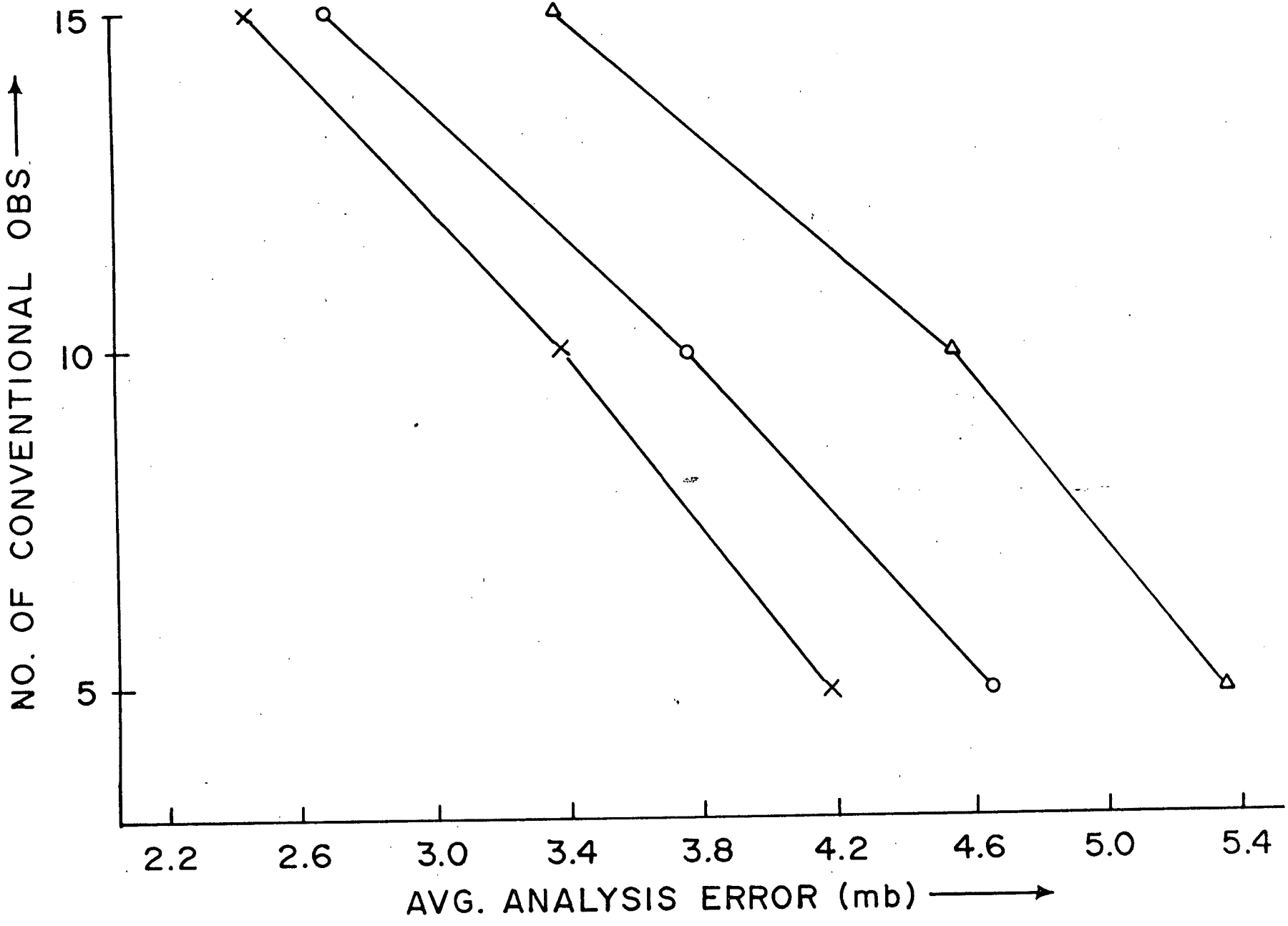
15
10
5
NO. OF CONVENTIONAL OBS
2.2
2.6
3.0
3.4
3.8
4.2
4.6
5.0
5.4
AVG. ANALYSIS ERROR (mb)

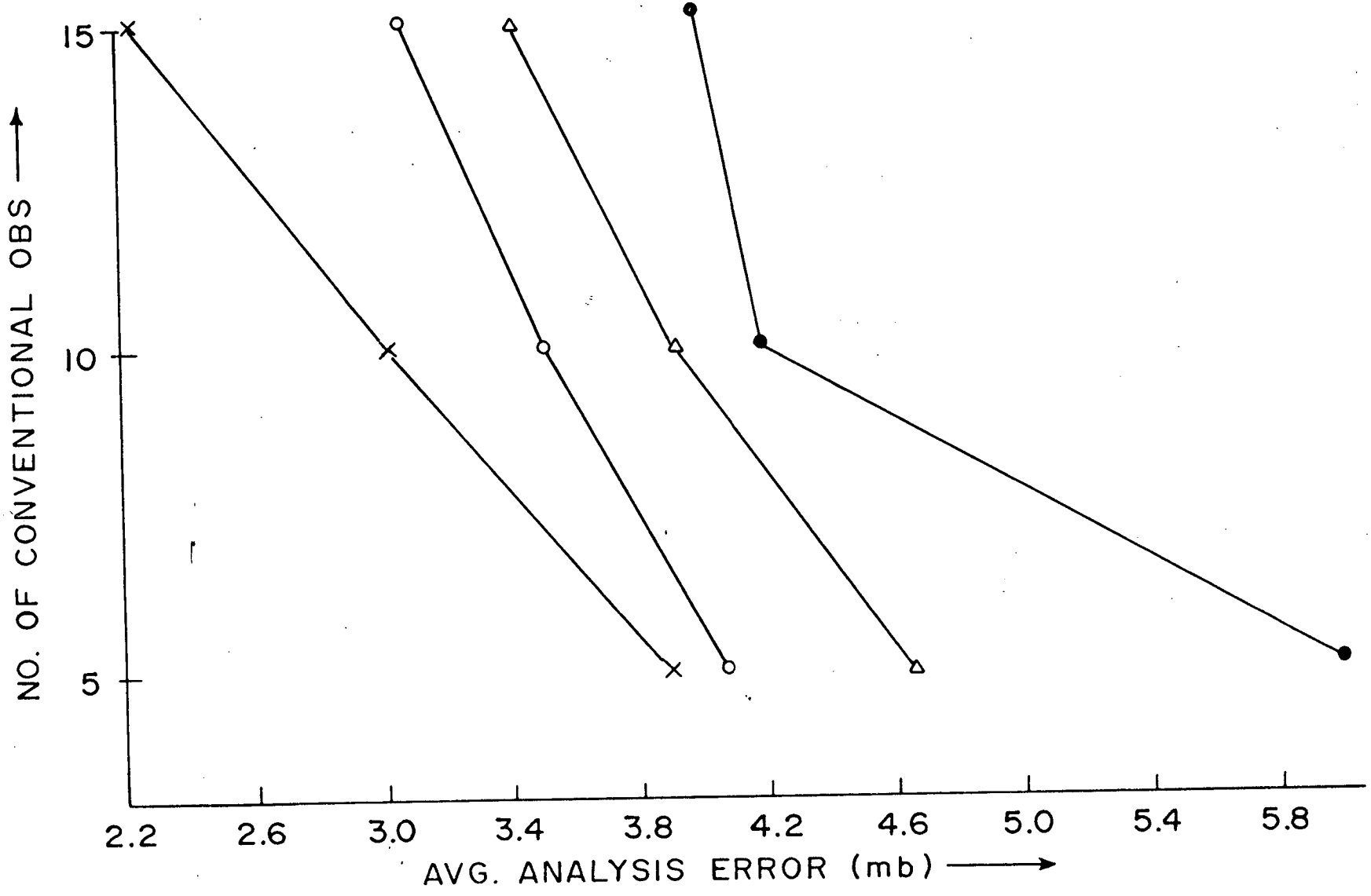
15
10
5
NO. OF CONVENTIONAL OBS
2.2
2.6
3.0
3.4
3.8
4.2
4.6
5.0
5.4
5.8
AVG. ANALYSIS ERROR (mb)